

## Alpha Particles Induced Modification on SSNTDs Stored for Long Time

A. F. Maged

*Department of Solid State and Electron Accelerator, NCRRT, Atomic Energy Authority, Nasr City, P.O. Box 29, Cairo, Egypt.*

**E**FFECTS of ageing on the optical properties of CR-39 SSNTDs were investigated for two stored types. The optical band gap of the stored pristine was roughly the same as the new pristine samples before chemical etching. Energy gaps were found to decrease with the chemical etching. The onset of the transmittance spectra of the CR-39 SSNTDs were measured at 240 nm and 300 nm for 26 y and 10 y respectively. The etch pit diameters of  $\alpha$ -particles were decreased with the storage period while the rate of the decrease depended markedly on the storage conditions. The fading effects of tracks due to radon exposure were a little bit changed. The storage at the temperature of 4 °C for 26 y did not bring any significant changes to the detection efficiency. These characterizations of the response of CR-39 SSNTDs to alpha particle were essential for the storage under certain conditions.

**Keywords:** CR-39 detectors, long-term storage, alpha particle, optical energy gap.

### Introduction

Solid state nuclear track detectors (SSNTDs) CR-39 are used widely in the field of health physics, such as for radon monitoring or neutron dosimetry. Authors used the CR-39 SSNTDs for  $\alpha$ -particle measurement and  $\alpha$ -particle autoradiography [Ishigure, 1985 and Ishigure et al., 1988]. Some results revealed that the ageing effect on CR-39 SSNTDs sensitivity is very strong this needs to be considered on the routine applications or research experiments. The authors noticed that the diameter of etch pits observed in CR-39 SSNTDs stored for a long time became smaller than those observed in a fresh plate of SSNTD CR-39. There were some reports about aging and/or fading effect of CR-39 SSNTDs. However, authors felt the necessity to examine more systematically the effect of aging and/or fading on the plates of CR-39 SSNTDs that were used by the authors themselves [Harrison, et al., 1986; Portwood et al., 1986; Fujii, et al., 1991; Csige, et al., 1991 and Hardcastle, et al., 1996]. The term "aging" is used for the change in the track registration property during storage until it is irradiated, while "fading" means the change in the track registration property during storage after irradiation. The 3-D imaging of particle

tracks in SSNTDs was investigated [Wertheim, et al., 2010]. The optical appearance of etched alpha-particle tracks in CR-39 SSNTDs under the transmission mode of the optical microscope was discussed [Law, et al., 2008].

Robu investigated the influence of exposure geometry on the response of CR39 SSNTDs radon detectors [Robu, et al., 2011]. UV-VIS spectral evaluation of CR-39 SSNTDs exposed with diagnostic dosage was studied by Nur Shadah, et al., [2014].

The bulk etch rate and the track etch rate of CR-39 SSNTDs were measured alpha particles emitted from radon gas in subsoil in various concentrations of NaOH in the range (6-8 Mole) at 70°C [Maged, and Ashraf, 1997].

In this study, the effect of long-term storage on CR-39 SSNTDs under certain conditions was investigated to study the ability of keeping all the information of tracks.

### Materials and Experiments

#### *CR-39 SSNTDs*

The detectors of CR-39 were purchased 26 y ago from Pershore Limited (Thickness, 500 $\mu$ m), UK and the others were purchased 10 y ago from

TASTRAK Thickness, 500 $\mu$ m), Bristol, UK. Before the start of the experiment, the sheet of CR-39 SSNTDs used was already stored in a refrigerator at 4 °C for 26 y and 10 y, respectively.

#### Storage of CR-39 SSNTDs

Sheets of CR-39 were enclosed one by one in polyethylene bags with zipper so that background due to radon progeny might not increase during the storage. The outside of the polyethylene bag was wrapped in aluminum foil to prevent the effect of ultraviolet radiation on the property of the CR-39 SSNTD.

#### Alpha source

The alpha source employed was a planar <sup>241</sup>Am source (activity was 741nCi and main alpha energy was 5.5 MeV in vacuum). The incidence of alpha particles was restricted to the chosen 90° incident angle in air with the help of a collimator. The schematic diagram of employed alpha source is shown in (Fig.1).

An aluminum plate of 3.0 mm in thickness, was used as a collimator to minimize the cross section of  $\alpha$ -source. One hole, 10.00 mm in diameter apart was drilled in the aluminum plate. The collimator was put on the radiation source directly. The resultant irradiation distance was 3.0 mm in the air. The irradiation time was 5 seconds.

#### Radon exposure

All data of counting were normalized according to the results of the 1997 European Commission Intercomparison of Passive Radon Detectors in UK through the Egyptian participation No.31 [EUR, 1998].

#### Chemical etching

After irradiation, the detectors were etched in a 6M aqueous solution of NaOH for different etching time until reaching to 18 h at 70 °C. The temperature was kept constant by a water bath with an accuracy of  $\pm 1$  °C. The detectors were then taken out from the etchant and rinsed with distilled water immediately in order to stop the reaction between the detectors and the etchant. The detectors were dried completely and then used for analysis [Maged et al., 1993].

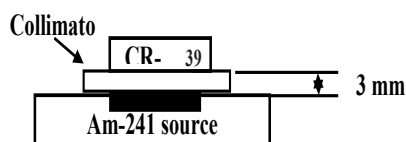


Fig 1. Schematic diagram of the experimental arrangement used to irradiate CR-39 SSNTDs.

Egypt. J. Rad. Sci. Applic., Vol. 30, No. 2(2017)

#### Optical microscope

An optical microscope operated in the transmission mode was used for observation of tracks. The images were recorded in the JPEG format by a digital camera (Samsung SAC 2300) installed on the microscope (Olympus BX60). The average area of one hundred fields of view was calculated using an image analysis system and the track density was calculated in terms of tracks.cm<sup>-2</sup>. The background track density was determined by processing a pristine detector under the same etching conditions. The background was subtracted from the measured track density.

#### Measurement of track dimension

The track dimensions were determined by the Quantimet 500 software. Calibration was carried out before measurements. An image of a calibration ruler (0.01mm per division) was used under the microscope and used for scale setting and calibration.

#### UV-VIS spectrophotometer

The optical transmittance spectra of the CR-39 detector were measured in the wavelength range from 190 to 1100 nm by means of the Specord 210 plus UV-VIS spectrophotometer (Made in Germany).

#### Interpretation of optical characterization

In order to understand the optoelectronic and photonic device behavior, it is good to first understand the optical properties of polymeric material. The optical properties of polymeric materials imply the electronic structure which affects the electrical and optical output in properties of optoelectronic and photonic. An absorption spectrum was a fingerprint of a molecule or a polymer material. UV-VIS absorption was a commonly used analytical tool for studying the interactions between electrons and radiation. The simplest method to investigate the electronic structure of a solid material was performed by studying its optical absorption. Absorption occurs when a photon has sufficient energy to excite electrons from the lowest energy to the highest energy. The fundamental equation between the absorption and optical energy gap  $E_{opt}$  was given by  $E_{opt} = \hbar\omega$ , where  $\omega$  was the light frequency and  $\hbar$  is the Planck constant. The fundamental absorption refers to a band-to-band transition in the solid phase. In crystalline materials, a direct transition occurs when electrons were excited from the valence band to the conduction band in the same  $k$ -space. In this process, the total energy and momentum were conserved. For indirect

transition, electrons cross the conduction band at different  $k$ -spaces. In this case, transition was possible only when phonon assisted. Given that the potential well fluctuates in amorphous materials, there was no specific definition in  $k$ -space (non-conservation of  $k$ -space) and electron localization occurs [Anderson, 1975]. According to the Mott-Davis model, the wave function was localized and the probability of transition depends on wave function overlapping [Mott, and Davis, 1968]. Considering that amorphous materials lack a long-range order, a localized state extends from the conduction and valence bands to the band gap. This localized state can affect the electron transition in amorphous and polymeric materials. The absorption coefficient  $\alpha$  was related to the absorbance  $A$  based on the Lambert-Beer law as follows;

$$\alpha = 2.303 A/t \quad (1)$$

where  $t$  was the sample thickness. The optical absorption for non-crystalline materials was given in previous studies [Wood, and Tauc, 1972; Mott, and Davis, 1971],

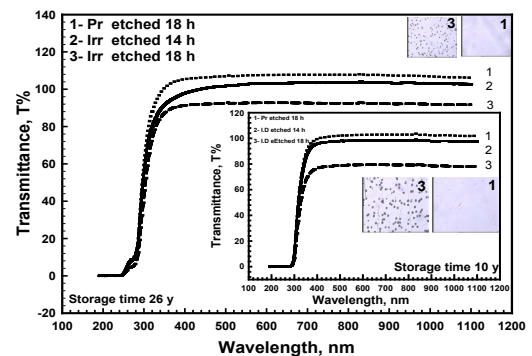
$$(\alpha \hbar \omega)^n = \beta (\hbar \omega - E_{opt}) \quad (2)$$

where  $\beta$  is a constant,  $E_{opt}$  is an optical energy gap and  $n$  was the exponential constant index. The exponential constant index is an important parameter that describes the type of electronic transition. There were four types of transition in amorphous materials that can be represented with  $n$ . The values of  $n$  were commonly 1/3, 1/2, 2/3, and 2 for indirect forbidden, indirect allowed, direct forbidden, and direct allowed transitions, respectively [Alias et al., 2012; Hassan et al., 2015].

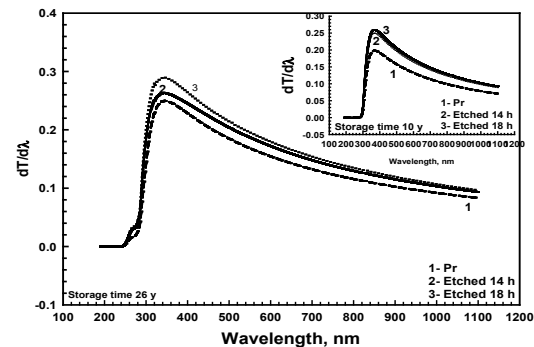
## Results And Discussion

The existence of the absorption edge and its shifting as a result of storage time of CR-39 SSNTDs were discussed. The indirect band gap of the pristine and irradiated CR-39 SSNTDs was determined. A decrease in the optical energy gap with the chemical etching was noticed for 10 y and 26 y. It could be discussed on the basis of alpha particles induced defects in forbidden gap of the CR-39 SSNTDs and also, due to the decrease in detector thickness. The transmittance spectra of the CR-39 SSNTD were taken to investigate the behavior of their optical properties with the two storage times and the plot of the transmittance vs. wavelength was shown in Fig.2a. The onset of the transmittance spectra of the CR-39 SSNTDs

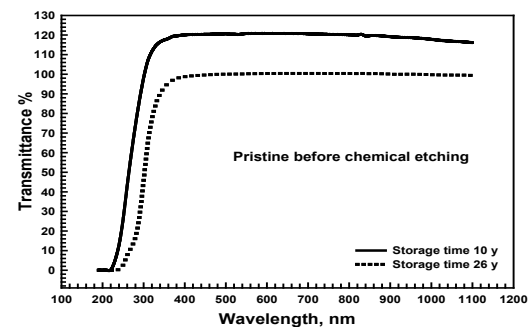
were measured at 240 nm and 300 nm for 26 y and 10 y respectively. The transmittance spectra of the CR-39 SSNTDs were sharply increased in the wavelength ranges of 240-350 nm and 300-400 nm for 26 y and 10 y respectively. After the wavelengths of 350 nm and 400 nm for 26 y and 10 y respectively, the transmittance spectra of the CR-39 SSNTDs were not again observed due to the high transparency in visible range. It was only noticed that a small peak at 250 nm was found after chemical etching for storage time 26 y and it might be due to annealing as shown in (Fig. 2a-c).



(a)



(b)



(c)

Fig. 2. (a). The plot of the transmittance vs.  $\lambda$ , (b) the curves of  $dT/d\lambda$  vs.  $\lambda$  of CR-39 SSNTDs after chemical etching and (c) The plot of the transmittance vs.  $\lambda$  of pristine before chemical etching (Pr: pristine, Irr: irradiated CR-39 SSNTDs).

The average transmittance ( $T_{avg}$ ) values of the CR-39 SSNTDs for 10 y and 26 y were calculated. The  $T_{avg}$  was measured 120% and 99% for pristine SSNTDs for 10 y and 26 y, respectively before chemical etching and no irradiation as shown in Fig.2c and Table 1. The lowest value of  $T_{avg}$  was measured 71% for storage time 10 y at chemical etching 18 h. Generally, it was observed, that the average transmittance values of the CR-39 SSNTDs in the visible region decrease with the increase of etching time as shown in Fig.2a. To estimate the absorption band edge of the CR-39 SSNTDs, the first derivative of the optical transmittance was computed. For this purpose, the curves of  $dT/d\lambda$  vs. wavelength of the CR-39 SSNTDs were plotted, as shown in Fig. 2b. The maximum peak values of the CR-39 SSNTDs vary from a wavelength 335 to 382 nm as shown in Table 1. The absorption band edge values of the CR-39 SSNTDs were calculated from the maximum peak position as given in Table 1.

These results explained that the absorption band edge of the CR-39 SSNTDs decreased with the chemical etching. The optical band gap of the CR-39 SSNTDs, the  $(\alpha \hbar\omega)^{1/2}$  plot vs. the photon energy E of the CR-39 SSNTDs was shown in Fig.3.

As seen in Fig.3, there was a linear region for the optical band gap  $E_{opt}$  values of the CR-39 SSNTDs. By extrapolating the linear plot to  $(\alpha \hbar\omega)^{1/2} = 0$ , the  $E_{opt}$  values of the CR-39 SSNTDs were obtained as given in Table 1. The highest and lowest values of  $E_{opt}$  were found 4.20 eV and 3.80 eV for 26 y and 10 y, respectively before chemical etching. These values of the CR-39 SSNTDs of pristine were found to be in rough agreement with the value 4.05 eV in the literature, [Nur Shadah, et al., 2014]. This result suggests that the optical band gap of the CR-39 detector was roughly stable with the storage time for long periods before chemical etching under keeping in certain conditions. It was shown previously that the CR-39 SSNTDs response to charged-particles drops sharply within the first 30 days of manufacture, [Cartwright, 1978] and that it was the age of the plastic itself, not of the tracks, which results in the degradation of sensitivity (lower  $V_T/V_B$ ) with time [Portwood et al., 1986]. The effects of prolonged aging on the CR-39 SSNTDs were studied using  $\sim 5.5$  MeV alpha particles from a  $^{241}\text{Am}$  source and samples over a 5-year period. After exposure, samples were stored in a low-humidity, low-light environment and at room temperature for a

**TABLE 1. The  $T_{avg}$  (in absorption region),  $\lambda_{max\ peak}$ , absorption band edge, optical energy gap  $E_{opt}$  values of the CR-39 SSNTDs after chemical etching.**

| Etching Time (hr) | $T_{avg}$ (%)                  |                                | $\lambda_{max\ peak}$ (nm)     |                                | Absorption band edge (eV) |                   | $E_{opt}$ (eV)    |                   |
|-------------------|--------------------------------|--------------------------------|--------------------------------|--------------------------------|---------------------------|-------------------|-------------------|-------------------|
|                   | Storage time 10 y <sup>T</sup> | Storage time 26 y <sup>P</sup> | Storage time 10 y <sup>T</sup> | Storage time 26 y <sup>P</sup> | 10 y <sup>T</sup>         | 26 y <sup>P</sup> | 10 y <sup>T</sup> | 26 y <sup>P</sup> |
| Pr (0 hr)         | 120                            | 99                             | 370                            | 345                            | 3.97                      | 3.98              | 4.10              | 4.20              |
| Pr (18 hr)        | 100                            | 100                            | 365                            | 342                            | 3.80                      | 3.88              | 3.80              | 4.10              |
| 14 (Irr.)         | 95                             | 91                             | 365                            | 342                            | 3.80                      | 3.86              | 3.80              | 4.05              |
| 18 (Irr.)         | 71                             | 85                             | 365                            | 342                            | 3.80                      | 3.85              | 3.80              | 4.00              |
| Avg.              | 97                             | 94                             | 366                            | 343                            | 3.84                      | 3.89              | 3.88              | 4.09              |
| S.D.              | 20                             | 7                              | 3                              | 2                              | 0.09                      | 0.06              | 0.15              | 0.09              |

Pr: pristine (unirradiated); Irr.: irradiated & etching; T: TASTRAK; P: Page Mouldings; Avg.: average; S.D: standard deviation.

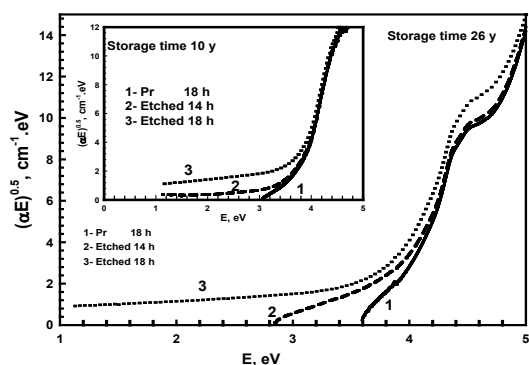


**Fig. 3. The  $(\alpha E)^{1/2}$  plot vs. the photon energy, E of CR-39 SSNTDs for two storing times**

*Egypt. J. Rad. Sci. Applic.*, Vol. 30, No. 2(2017)

variable amount of time, after which they were etched using the standard 6 N solution of NaOH at 80 °C for 6 hours [Portwood et al., 1986]. To determine whether it was the age of the plastic or the age of the track which causes a reduction in track diameter, another set of samples which was previously exposed to alpha particles was exposed again immediately before etch. The ratios of diameters of the old alpha tracks to the new alpha tracks was unity to within 5%, suggesting that it was the age of the CR-39 SSNTDs, not the age of the track, which was responsible for the reduction in diameter. These results are in agreement with previous claims utilizing

different materials [Portwood et al., 1986]. The cause for the observed change in response may be annealing [Bhatia et al., 1990] or oxidation [Portwood et al., 1986]. Given the experimental setup, we rule out long-term exposure to UV and humidity. It was shown that storing CR-39 SSNTDs at or below freezing temperatures will inhibit these aging effects [Portwood, et al., 1986; Sinenian, et al., 2012 and Matiullah, et al., 2005]. High inherent sensitivity of CR-39 to detect relatively lower-LET particles, proved efficacy of 50 Hzeri (high voltage) electrochemical etching method and need to efficient alpha detection methods prompted was investigated [Sohrabi, and Soltani, 2017]. The results proved that the contribution of high LET secondary particles to the dose characteristics for 9.6 and 30.0 MeV proton energies were more significant as compared to their contribution at higher proton energies [Spurn'y et al., 2001]. This phenomenon could be imperative in such fields as radiotherapy, radiobiology, and radiation protection. As far as proton radiotherapy and proton radiobiology studies are concerned, the dose due to secondary high LET charged particles changes not only quantitative, but also qualitative characteristics of the beam. Since the contribution of the secondary charged particles to the absorbed dose at the beam entrance at 9.6 and 30.0 MeV energies were more significant, the absorbed dose would increase substantially at greater depths. Besides, due to the increased percentage of high LET particles, radiobiological characteristics of the beam may

also change with the depth [Ghergherehchi, et al., 2008]. Maged et al investigated both of the environmental risk assessment of radon from ceramic tiles in Egypt, estimating the radon concentration in water and indoor air and radon concentration in elementary schools in Kuwait by using CR-39 track detectors [28-30] [Maged, et al., 2012; Maged, 2009 and Maged, 2006]. Our studies were extended to include the track density, the track dimension, orientation and roundness response of alpha particles from  $^{241}\text{Am}$  source of energy  $\sim 5.5$  MeV and from alpha particles emitted from radon exposure since 1997 via sharing in radon Intercomparison [EUR, 1998] as shown in Tables 2-3. The CR-39 SSNTDs in Table 2 were etched for 18 hours in a 6 M solution of NaOH at  $70^\circ\text{C}$ . Table 2 shows that the alpha track length and breadth, perimeter, were decreased with the increase of storage time at the same chemical conditions. The track density was found to be roughly the same. The roundness was increased with storage time. When CR-39 SSNTDs used for radon monitoring or neutron dosimetry, the following points should be recommended to: (1) the detector should be stored in a refrigerator at  $4^\circ\text{C}$  before exposure and until etching after the exposure, (2) the change in the sensitivity between the time of calibration and the time of use should be evaluated and the counting efficiency at the measurement should be corrected and (3) for comparison or for interpretation of experimental results in different experiments the effect of storage should be carefully considered.

TABLE 2. Aging of CR-39 detectors were stored at  $4^\circ\text{C}$ .

| Storage time (year)   | $\rho$<br>(tracks density) | L<br>( $\mu\text{m}$ ) | B<br>( $\mu\text{m}$ ) | P<br>( $\mu\text{m}$ ) | O             | R               |
|-----------------------|----------------------------|------------------------|------------------------|------------------------|---------------|-----------------|
| 10 (TASTRAK)          | $2.3 \times 10^4 \pm 10\%$ | $37 \pm 11\%$          | $26 \pm 6\%$           | $131 \pm 54\%$         | $62 \pm 95\%$ | $1.87 \pm 57\%$ |
| 26 (Pershore Limited) | $2.2 \times 10^4 \pm 15\%$ | $16 \pm 12\%$          | $12 \pm 12\%$          | $66 \pm 24\%$          | $30 \pm 80\%$ | $2.4 \pm 19\%$  |

L: The length of the longest feret B: The length of the shortest feret Feret diameter: caliper diameter

P: The total length of the boundary of the feature (track).

O: Orientation

R: Roundness

TABLE 3. Fading of tracks due to radon exposure stored in refrigerator at  $4^\circ\text{C}$  since 1997 [13].

| Στοραγε τιμε<br>( $\psi\epsilon\alpha\rho$ ) | $\rho$<br>(tracks density)  | L<br>( $\mu\text{m}$ ) | B<br>( $\mu\text{m}$ ) | P<br>( $\mu\text{m}$ ) | O             | R               |
|----------------------------------------------|-----------------------------|------------------------|------------------------|------------------------|---------------|-----------------|
| 19 (Pershore)                                | $3.12 \times 10^2 \pm 15\%$ | $29 \pm 2\%$           | $24 \pm 1\%$           | $110 \pm 11\%$         | $72 \pm 45\%$ | $1.8 \pm 0.3\%$ |

For fading study; the samples stored at 4 °C of “Results of the 1997 European Commission Intercomparison of Passive Radon Detectors” [EUR, 1998] No. 31, were found roughly the same after 19 years of storage time as reported in Table 3.

### Conclusions

The optical band gap of the stored pristine was roughly the same as the new pristine samples before chemical etching. By the conventional method, we obtained  $E_{opt}$  of ~4.1 eV before chemical etching under the assumption that all the films consisted of amorphous phase. The etch pit diameters of  $\alpha$ -particles were decreased with the storage period and the rate of that decrease depended markedly on the storage conditions. The bulk etch rate at 4 °C was slightly changed with the storage period. The storage at 4 °C for 26 y did not result in significant changes to the detection efficiency. The fading effects of tracks due to radon exposure after 19 y storage changed slightly. These characterizations of the response of CR-39 SSNTDs to alpha particle were essential for the storage under certain conditions.

### References

- Alias, A. N. , Kudin, T. T. I., Zabidi, Z. M., Harun, M.K. and Yahya, M. Z. A. (2012) Optical Characterization of Luminescence Polymer Blends Using Tauc/Davis-Mott Model. *Advanced Materials Research*, **488**, 628.
- Anderson, P. W. (1975) Model for the electronic structure of amorphous semiconductors. *Physical Review Letters* **34**, 953.
- Bhatia, R. K. , Singh, R. C. and Virk, H. S. (1990) Anomalous behavior of environment affected CR-39 at elevated temperatures. Nuclear Instruments and Methods in Physics Research Section B: Beam Interactions with Materials and Atoms, **46**, 358.
- Cartwright, B. G. , Shirk, E. K. and Price, P. B. (1978) A nuclear-track-recording polymer of unique sensitivity and resolution. *Nuclear Instruments and Methods*, **153**, 457.
- Csige, I. , Hunyadi, I. and Charvat, J. (1991) Environmental Effects on Induction Time and Sensitivity of Different Types of CR-39. *Nucl. Tracks & Radiat. Meas.*, **19**, 151.
- EUR 1803, (1998) Results of the 1997 European Commission Intercomparison of Passive Radon Detectors, ISSN: 1018-5593 EN.
- Egypt. J. Rad. Sci. Applic., Vol. 30, No. 2(2017)
- Fujii, M. , Yokota, R. , Kobayashi, T. and Hasegawa, H. (1991) Ageing Effects in Polymeric Track Detectors. *Housyasen*, **18**, 4.
- Ghergherehchi, M. , Afarideh, H. , Ghanadi Maraghe, M. , Mohammadzadeh, A. and Esmailnezhad, M. (2008) Proton beam dosimetry by CR-39 track-etched Detector”. *Iran. J. Radiat. Res.*, **6** (3), 113.
- Harcastle, G. D. and Miles, J. C. H. (1996) Ageing and Fading of Alpha Particle Tracks in CR-39 Exposed to Air. *Radiat. Protec. Dosim.*, **67**, 295.
- Harrison, K.G., Haigh, R.M. and Goodenough, R. (1986) Some Studies of the Neutron Response, Background, Ageing and Fading Properties of Two Different Types of CR-39 Plastic Processed by Electrochemical Etching. *Nucl. Tracks & Radiat. Meas.*, **12**, 653.
- Hassan, M. J. A., Yusoff, M. A. and Vengadesh, P. (2015) Calculation of the Electronic Parameters of an Al/DNA/p-Si Schottky Barrier Diode Influenced by Alpha Radiation. *Sensors (Basel)*. **15**, 4810.
- Ishigure, N. (1985) Application of CR-39 Plastic to Rapid and Quantitative Macro-autoradiography of  $\alpha$ -Emitters in a Whole Body Section of an Experimental Animal. *Radioisotopes*, **34**, 101.
- Ishigure, N. and Matsuoka, O. (1988) Factors Affecting Etching Properties of CR-39 Detector for Alpha-Particles. *J. Nucl. Sci. Technol.*, **25**, 404.
- Law, Y. L., Nikezic, D and Yu, K. N. (2008) Optical appearance of alpha-particle tracks in CR-39 SSNTD. *Radiat. Meas.*, **43**, S128.
- Maged, A. F. Tsuruta, T. and Durrani, S. A. (1993) Experimental and theoretical considerations on the calibration factor K between  $\alpha$ -activity concentration and track density for application in radon dosimetry. *J. Radioanalyt. Nucl. Chem.*, **170**, 423.
- Maged, A.F., Lotfi Z. Ismail and Nada .L.A. Moussa (2012) Environmental risk assessment of radon from ceramic tiles. *Radioprotection*, **47**, 3, 403.
- Maged, A.F. (2009) Estimating the radon concentration in water and indoor air. *Environmental Monitoring and Assessment*, **152**, 195.
- Maged, A. F. (2006) Radon Concentration in Elementary Schools in Kuwait. *Health Physics*, **90**, 3,258.

- Maged, A. F. and Ashraf, F. A. (1997)** Effect of various etching conditions on the response of Cr-39 plastic track detector applied for radon dosimetry in environment. First Arabic Conference of Applied Chemistry (Chemistry in Development Service) Cairo 1-5, 567. [www.iaea.org/inis/collection/NCLCollectionStore/\\_Public/29/038/29038068.pdf](http://www.iaea.org/inis/collection/NCLCollectionStore/_Public/29/038/29038068.pdf).
- Matiullah, Rehman, S. , Rehman, S. and Zaman, W. (2005)** Discovery of new etchants for CR-39 Detector, *Radiat. Meas.*, **39**, 337.
- Mott, N. F. and Davis, E. A. (1968)** Conduction in non-crystalline systems. *Philosophical Magazine*, **17**, 1269.
- Mott, N. F. and Davis, E. A. (1971)** Electronic Processes in Non-Crystalline Materials. London: Oxford University Press.
- Nur Shadah, Z. , Iskandar, S. M. , Azhar, A. R. , Suhaimi, M. J. , Nur Lina, R. and Halimah, M. K. (2014)** UV-VIS Spectral Evaluation of CR-39 Detector Exposed with Diagnostic Dosage. *Sains Malaysiana*, **43**, 953.
- Portwood, T. , Henshaw, D. L. and Stejny, J. (1986)** Ageing effects in CR-39. Inter J. Radiat. Appl. and Instrum. Part D. Nucl. Tracks & Radiat. Meas., **12**, 109.
- Robu, E. , Maringer, Garavalia, F. J. M. and Picini, L. (2011)** Influence of exposure geometry on the response of CR39 SSNT Radon Detectors. *Romanian Reports in Physics*, **63**, 376.
- Sinenian, N. , Rosenberg, M. J. , Manuel, M. J. E. , McDuffee, S. C. , Casey, D. T. , Zylstra, A. B. , Rinderknecht, H. G. , Johnson, M. G. , Seguin, F. H. , Frenje, J. A. and Li, C. K. (2012)** The response of CR-39 nuclear track detector to 1-9 MeV protons. Petraso RD, PSFC/JA-11.
- Spurn'y F, Bamblevski VP, Molokanov AG and Vleck B (2001)** Dosimetric and microdosimetric characteristics of high energy proton beams. *Radiation Measurement*, **34**, 527.
- Sohrabi, M. and Soltani, Z. (2017)** Alpha particle energy response of CR-39 detectors by 50 Hz–HV electrochemical etching method. *Results in Physics*, **7**, 69.
- Wertheim, D., Gillmore, G. , Brown, L. and Petford, N. (2010)** 3-D imaging of particle tracks in solid state nuclear track detectors. *Nat. Hazards Earth Syst. Sci.*, **10**, 1033.
- Wood, D. L. and Tauc, J. (1972)** Weak Absorption Tails in Amorphous Semiconductors. *Physical Review B*, **5**, 3144.

(Received 19/1/2017;  
accepted 4/12/2017)

## التغيرات التي تحدث في كواشف الأثر النووي المعرضة لجسيمات ألفا المخزنة لفترة زمنية طويلة

ماجد على فهمي

قسم الجوامد و المعجلات الألكترونية - المركز القومي لبحوث وتكنولوجيا الإشعاع - هيئة الطاقة الذرية

دراسة تأثير التخزين على الخواص الفيزيائية لكواشف الأثر النووي سي ار-39 لنوعين لهذا الكاشف. تبين أن حزمه الفجوه الضوئية للكاشف المخزن لها تقريبا نفس الصفات للكاشف الجديد قبل عملية الحفر الكيميائي. لقد وجد أن فجوه الطاقه تتناقص مع الحفر الكيميائي. لقد تم قياس بدايه أطياف النفاذيه الضوئية للكواشف عند أطوال موجيه ٢٤٠ نانومتر و ٣٠٠ نانومتر لفترة تخزين ٢٦ سنه و عشر سنوات على التوالي. لقد تناقص قطر الأثر النووي الناتج من جسيمات الفا بعد الحفر الكيميائي مع فترة التخزين و حيث أن معدل التناقص قد اعتمد على ظروف التخزين. تأثيرات فقد الأثار النوويه نتيجة التعرض للرادون كانت قليلة جدا. تخزين الكواشف لمدة ٢٦ سنه في درجه حراره ٤ مئوية لم تظهر تغيرات ذات اهميه لكفائه الكاشف. أستجابته هذه الخصائص بعد التخزين لكواشف الأثر النووي بالنسبه لجسيمات الفا يكون ضروريا أن تخزن في ظروف معينه.